

# Chiral Two-Body Bound States from Berry Curvature and Chiral Superconductivity

Daniil Karuzin<sup>1</sup> and Leonid Levitov<sup>2</sup>

<sup>1</sup>*Moscow Institute of Physics and Technology, Dolgoprudny 141701, Russia*

<sup>2</sup>*Department of Physics, Massachusetts Institute of Technology, Cambridge MA02139, USA*

Motivated by the discovery of exotic superconductivity in rhombohedral graphene, we study the two-body problem in electronic bands endowed with Berry curvature and show that it supports chiral, non-*s*-wave bound states with nonzero angular momentum. In the presence of a Fermi sea, these interactions give rise to a chiral pairing problem featuring multiple superconducting phases that break time-reversal symmetry. These phases form a cascade of chiral topological states with different angular momenta, where the order-parameter phase winds by  $2\pi m$  around the Fermi surface, with  $m = 1, 3, 5, \dots$ , and the succession of phases is governed by the Berry-curvature flux through the Fermi surface area,  $\Phi = bk_F^2/2$ . As  $\Phi$  increases, the system undergoes a sequence of first-order phase transitions between distinct chiral phases, occurring whenever  $\Phi$  crosses integer values. This realizes a quantum-geometry analog of the Little–Parks effect—oscillations in  $T_c$  that provide a clear and experimentally accessible hallmark of chiral superconducting order.

The interplay between superconductivity and magnetic fields is a classic example of how, in Aristotle’s words, “the whole is greater than the sum of its parts”: two seemingly antagonistic tendencies combine to produce a vast array of vortex-bearing superconducting phases with emergent properties unavailable to either ingredient alone [1–5]. Here we will be interested in a quantum-geometry variety of vortical superconductivity with vorticity occurring in  $k$  space rather than in the coordinate space, being induced by, and intertwined with, a pseudomagnetic field encoded in the Berry curvature of the electronic bands [6–12]. This interest is motivated by recent observations of chiral superconductivity in valley-polarized rhombohedral graphene multilayers [17] and associated theoretical proposals for topological superconductivity in rhombohedral tetra- and pentalayer graphene [10, 18–22]. As many authors pointed out [10, 18–22], the Berry curvature has a profound impact on individual chiral superconducting phases.

Here, we develop a microscopic framework for this physics using a simple, exactly solvable model of a single band with Berry phase. The phase diagram shows a clear sequence of chiral phases with related topological properties, controlled by the commensurability between the Berry-curvature flux and the Fermi-surface area, as illustrated in Fig. 1. First-order transitions between these phases produce a “quantum-geometric” Little–Parks-like effect, seen as oscillations of the critical temperature  $T_c$  as a function of Berry-phase flux.

It is instructive to draw a comparison with conventional type-II superconductors, where vortices induced by magnetic fields do not fundamentally alter the microscopic structure of the paired state; their main effect is to generate vortex phases and impact the long-range order of the system. By contrast with the conventional case, Berry curvature directly influences pairing type and symmetry on microscales. Berry-curvature-induced pseudomagnetic fields also drive transitions between distinct topological superconducting phases, in which the order-parameter phase winds in momentum space and the superconducting state acquires nontrivial topology [10, 13–

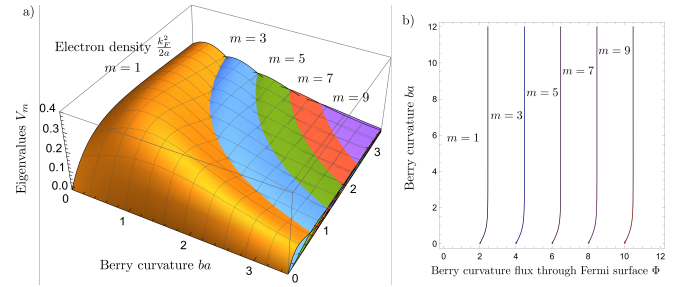


FIG. 1. (a) Hierarchy of chiral pairing channels from the chiral two-body interaction, Eq. (4), controlled by commensurability of the Berry-curvature flux  $\Phi$ , Eq. (23), and the Fermi-surface area. Plotted are eigenvalues of the linearized gap equation, Eq. (12), versus Berry curvature  $b$  and carrier density  $k_F^2/4\pi$ , measured in units of  $1/a$  and  $a/2\pi$ , respectively. The 3D surfaces show the leading (maximal) eigenvalues, labeled by angular-momentum quantum numbers  $m = 1, 3, 5, 7, \dots$ . Phase boundaries  $V_m = V_{m+2}$  between different  $m$  are well approximated by the hyperbolae  $bk_F^2/2 = \sqrt{(m+1)(m+2)}$ . (b) The same phase boundaries  $V_m = V_{m+2}$  in terms of flux  $\Phi$ , which occur near half-integer  $\Phi$  at small  $b$  and near integer  $\Phi$  at large  $b$ .

15]. Such phases are expected to exhibit strong orbital magnetism, host exotic (Majorana) quasiparticles and chiral edge excitations, and display anomalous thermal transport and related signatures [13–16]. The goal of this work is to elucidate how Berry curvature reshapes the phase diagram of superconductors, promoting chiral, time-reversal-breaking states even in the absence of any applied magnetic field.

To understand the key aspects of the chiral pairing problem, it is instructive to first consider the chiral two-body problem

$$H_{12} = \frac{\mathbf{p}_1^2}{2m} + \frac{\mathbf{p}_2^2}{2m} + V(\mathbf{R}_1 - \mathbf{R}_2), \quad \mathbf{R}_j = \mathbf{r}_j + \mathbf{a}(\mathbf{k}_j), \quad (1)$$

where  $\mathbf{a}(\mathbf{k}) = i\langle u_{n\mathbf{k}} | \nabla_{\mathbf{k}} u_{n\mathbf{k}} \rangle$  is the Berry connection of band  $n$ ;  $\mathbf{R}_j$  denote covariant particle coordinates [6, 7].

It is convenient, owing to translation symmetry, to work in the momentum representation,  $\mathbf{p}_j \rightarrow \mathbf{p}_j$ ,  $\mathbf{r}_j \rightarrow$

$i\hbar\partial_{\mathbf{p}_j}$ ,  $j = 1, 2$ , and use the center of mass frame, introducing relative coordinates and momenta

$$\mathbf{r} = \mathbf{r}_1 - \mathbf{r}_2, \quad \mathbf{p} = (\mathbf{p}_1 - \mathbf{p}_2)/2. \quad (2)$$

The two-particle Hamiltonian in the center of mass frame  $\mathbf{p}_1 + \mathbf{p}_2 = 0$  takes the form of a one-particle Hamiltonian for a particle with a reduced mass  $\mu = m/2$ :

$$H_{12} = \frac{\mathbf{p}^2}{2\mu} + V(\mathbf{R}_1 - \mathbf{R}_2), \quad \mathbf{R}_j = i\partial_{\mathbf{k}_j} + \mathbf{a}(\mathbf{k}_j). \quad (3)$$

To simplify algebra, below we specialize to the pairing interaction of a Gaussian form

$$V(\mathbf{R}_1 - \mathbf{R}_2) = \lambda e^{-a(\mathbf{R}_1 - \mathbf{R}_2)^2}, \quad \lambda < 0, \quad (4)$$

and choose Berry connection describing a uniform pseudomagnetic field

$$\mathbf{a}(\mathbf{k}) = \frac{bk}{2} \mathbf{e}_\varphi = \frac{1}{2}b(k_y, -k_x). \quad (5)$$

We note that the Gaussian model can be readily generalized to an arbitrary distance dependence of the pairing interaction by writing the interaction as a sum (or, integral) of gaussian contributions with different  $a$ . The uniform  $b$ -field approximation provides a toy model that allows an analytic solution and captures the essential aspects of the problem of chiral bound states and chiral superconductivity. Generalization to a more general Berry curvature is, in principle, straightforward.

In our model, the interaction depends on a parameter  $a$  characterizing the interaction radius  $1/\sqrt{a}$ . While the solution given below is applicable to any  $a$ , some of the essential physics will depend on the relation between the radius  $1/\sqrt{a}$  and  $\lambda_F$ , allowing this model to capture different regimes of interest.

Next, we demonstrate how eigenvalues and eigenstates of the chiral two-particle problem can be obtained in a closed form. To that end, we consider the operator

$$\mathbf{R}^2 = \left( i\partial_{\mathbf{k}} + \frac{bk}{2} \mathbf{e}_\varphi \right)^2. \quad (6)$$

This quantity is nothing but the Hamiltonian of a non-relativistic particle in an external magnetic field, with eigenvalues  $\rho_{n,m} = b(2n + |m| + m + 1)$ . The spectrum of the problem  $V(\mathbf{R})|\psi\rangle = \epsilon^{(V)}|\psi\rangle$  is therefore

$$\epsilon_{n,m}^{(V)} = \lambda e^{-a\rho_{n,m}}, \quad (7)$$

and the corresponding eigenfunctions in momentum space can be written as

$$\begin{aligned} \psi_{n,m}(k, \varphi) &= b^{\frac{1+|m|}{2}} \sqrt{\frac{(|m|+n)!}{2^{|m|}n!|m|!}} \frac{e^{-im\varphi}}{\sqrt{2\pi}} \\ &\times e^{-\frac{bk^2}{4}} k^{|m|} {}_1F_1\left(-n, |m|+1, \frac{bk^2}{2}\right), \end{aligned} \quad (8)$$

where  ${}_1F_1$  denotes a confluent hypergeometric function.

We can add the kinetic energy as a perturbation  $p^2/2\mu$ . The selection rules imply  $m = m' \Rightarrow n = n'$ , so the perturbation is diagonal in the  $\{\psi_{n,m}\}$  basis. The levels  $\epsilon_{n,m}^{(V)}$  are then shifted by

$$\delta\epsilon_{n,m} = \frac{\hbar^2}{b\mu} (2n + |m| + 1), \quad (9)$$

which completely lifts the Landau-level degeneracy.

A more consequential effect of reinstating the kinetic energy is that the two-body problem now acquires a continuous spectrum. At large inter-particle separations, the kinetic term inevitably dominates, even if the interaction  $V$  is strong at short distances. As a result, the spectrum remains discrete only at negative energies, where the levels correspond to bound states induced by the pseudomagnetic field arising from the Berry curvature. Properties of these bound states is an interesting question that will be discussed elsewhere.

In contrast, at positive energies the Hamiltonian in Eq. (1) defines a scattering problem: the ‘in’ and ‘out’ states are plane waves describing the motion of two particles at asymptotically large separations. This scattering problem has distinctive features due to the influence of Berry curvature on the scattering dynamics.

Moving to discuss superconductivity in a 2D Fermi sea, we consider spinless fermions interacting through a quantum-geometric attractive pairing interaction

$$\begin{aligned} H &= \int d^2x \psi^\dagger(x) \left( \frac{\mathbf{p}^2}{2m} - \mu \right) \psi(x) + \frac{1}{2} \iint d^2x_1 d^2x_2 \\ &\psi^\dagger(x_2) \psi^\dagger(x_1) V(\mathbf{R}_1 - \mathbf{R}_2) \psi(x_1) \psi(x_2). \end{aligned} \quad (10)$$

This Hamiltonian can be viewed as a projection of a multiband Dirac-type Hamiltonian on a single band, where the coordinate-space long derivative structure  $\mathbf{R}_i = i\partial_{\mathbf{k}_i} + \mathbf{a}(\mathbf{k}_i)$  arises from projection in the adiabatic approximation[6, 7]. We stress that such quantum-geometry structure of the interaction is totally general, applicable to any band dispersion and any Berry connection distribution in  $k$  space.

For simplicity, in this model, we ignore spin and valley degrees of freedom. This framework is relevant for the rhombohedral graphene superconducting systems in which electrons are spin- and valley-polarized. Spin-triplet pairing mandates odd-parity angular momentum, limiting possible  $m$  values to  $m = 1, 3, 5, \dots$  Extending the model to include valley and spin would be straightforward.

In what follows, we analyze the scattering amplitude for this two-body problem in the presence of a Fermi sea, and compute the vertex function  $V_{\mathbf{k},\mathbf{k}'}$  describing pair-scattering processes  $(\mathbf{k}, -\mathbf{k}) \rightarrow (\mathbf{k}', -\mathbf{k}')$  that drive the pairing instability. As we will see, the attractive chiral interaction  $V$ , Eq.(7),  $\lambda < 0$ , leads to paired state with angle dependent pairing interaction, described by

$$H = \sum_{\mathbf{k}} \xi_{\mathbf{k}} c_{\mathbf{k}}^{\dagger} c_{\mathbf{k}} + \sum_{\mathbf{k}} \Delta^*(\mathbf{k}) c_{-\mathbf{k}} c_{\mathbf{k}} + \Delta(\mathbf{k}) c_{\mathbf{k}}^{\dagger} c_{-\mathbf{k}}^{\dagger}, \quad (11)$$

where  $\Delta(\mathbf{k})$  obeys the gap equation

$$\Delta(\mathbf{k}) = - \sum_{\mathbf{k}'} V_{\mathbf{k},\mathbf{k}'} \frac{\Delta(\mathbf{k}')}{2E_{\mathbf{k}'}} \tanh\left(\frac{E_{\mathbf{k}'}}{2T}\right), \quad (12)$$

where  $E_{\mathbf{k}'} = \sqrt{|\Delta(\mathbf{k}')|^2 + \xi_{\mathbf{k}'}^2}$  and  $V_{\mathbf{k},\mathbf{k}'}$  is the two-particle scattering amplitude due to the chiral interaction  $V$ , Eq.(7). The angle dependence in  $V_{\mathbf{k},\mathbf{k}'}$  will lead to an array of different chiral phases.

To understand the properties of  $V_{\mathbf{k},\mathbf{k}'}$ , we consider the problem of two electrons scattering from the state  $(\mathbf{k}, -\mathbf{k})$  to the state  $(\mathbf{k}', -\mathbf{k}')$ . In the center-of-mass frame, Eq.(3), this process is governed by the scattering amplitude  $V_{\mathbf{k},\mathbf{k}'} = \langle \mathbf{k} | \lambda e^{-a\hat{R}^2} | \mathbf{k}' \rangle$ . Working in the Landau gauge, we write the quantity  $\hat{R}^2$  as

$$\mathbf{R}^2 = (i\partial_{k_x} - bk_y)^2 - \partial_{k_y}^2. \quad (13)$$

Since  $x$  is conserve, we can use the Fourier transform

$$V_{\mathbf{k},\mathbf{k}'} = \int dx e^{-i(k_x - k'_x)x} \tilde{V}_x(k_y, k'_y), \quad (14)$$

where  $\tilde{V}_x$  is a matrix element  $\langle k_y | \exp[-a\{(x - bk_y)^2 - \partial_{k_y}^2\}] | k'_y \rangle$ .

By making a substitution  $k_y \rightarrow k_y + \frac{x}{b}$ , we get  $\hat{R}^2 = b^2 k_y^2 - \partial_{k_y}^2$ . The matrix element  $\langle k_y | e^{-a(b^2 k_y^2 - \partial_{k_y}^2)} | k'_y \rangle$  can be calculated explicitly via 1D oscillator eigenstates

$$\begin{aligned} \langle k_y | e^{-a(b^2 k_y^2 - \partial_{k_y}^2)} | k'_y \rangle &= \sqrt{\frac{2\pi b}{\sinh(2ab)}} \\ &\times \exp\left[-\frac{b}{2\sinh(2ab)}((k_y^2 + k_y'^2) \cosh(2ab) - 2k_y k_y')\right]. \end{aligned} \quad (15)$$

Substituting back  $k_y \rightarrow k_y - \frac{x}{b}$  and integrating over  $x$ , we obtain the final answer

$$\begin{aligned} V_{\mathbf{k},\mathbf{k}'} &= \frac{\lambda\pi b}{\sinh(ab)} \exp\left[-\frac{b}{4} \coth(ab) (\mathbf{k} - \mathbf{k}')^2\right] \\ &\times \exp\left[-i\frac{b}{2}(k_y + k'_y)(k_x - k'_x)\right]. \end{aligned} \quad (16)$$

Importantly, the form of the vertex function depends on the choice of gauge  $\mathbf{a}(\mathbf{k})$ . To transform the result in the Landau gauge, Eq.(16), to the one in a symmetric gauge we perform a gauge transform for the electron wave functions,  $\mathbf{A} \rightarrow \mathbf{A} + \nabla f$ ,  $\psi \rightarrow \psi e^{if}$ . This yields

$$V_{\mathbf{k},\mathbf{k}'} \rightarrow V_{\mathbf{k},\mathbf{k}'} e^{if(\mathbf{k}) - if(\mathbf{k}')}. \quad (17)$$

By taking  $f = \frac{1}{2}bk_x k_y$ , we arrive at the answer in the symmetric gauge  $\mathbf{a} = \frac{1}{2}\mathbf{b} \times \mathbf{k}$

$$V_{\mathbf{k},\mathbf{k}'} = \frac{\lambda\pi b}{\sinh(ab)} \exp\left[-\frac{b}{4} \coth(ab) (\mathbf{k} - \mathbf{k}')^2 + i\frac{b}{2} e_z(\mathbf{k}' \times \mathbf{k})\right] \quad (18)$$

where  $e_z(\mathbf{k}' \times \mathbf{k})$  denotes a scalar associated with the vector cross product pointing out of plane.

To isolate contributions to pairing with different angular momenta, we can project  $V_{\mathbf{k},\mathbf{k}'}$  on the angular  $m$  harmonic on the Fermi surface. The angle dependence in  $V_{\mathbf{k},\mathbf{k}'}$  is given by

$$V(\phi_k - \phi_{k'}) \sim \exp[A \cos(\phi_k - \phi_{k'}) + iB \sin(\phi_k - \phi_{k'})], \quad (19)$$

where  $A = \frac{b}{2} \coth(ab) k_F^2$ ,  $B = \frac{b}{2} k_F^2$ . Denoting  $u = \frac{A+B}{2}$ ,  $v = \frac{A-B}{2}$ , we can rewrite the last equation as

$$V(\phi_k - \phi_{k'}) \sim \exp[ue^{i(\phi_k - \phi_{k'})} + ve^{-i(\phi_k - \phi_{k'})}]. \quad (20)$$

We expand this expression in terms of angular harmonics

$$V(\phi) = \sum_m V_m e^{im\phi}, \quad V_m = \int \frac{d\phi}{2\pi} V(\phi) e^{-im\phi}. \quad (21)$$

The values  $V_m$  are readily obtained by inverse Fourier transform, giving a closed-form expression:

$$V_m = \frac{\lambda\pi b}{\sinh(ab)} e^{-\frac{bk_F^2}{2} \coth(ab)} I_m\left(\frac{bk_F^2}{2\sinh(ab)}\right) e^{mab}. \quad (22)$$

The dependence of the quantities  $V_m$  on  $b$ ,  $k_F$  and parameter  $a$  characterizing the pair interaction potential width governs the hierarchy of the chiral states arising at different electron densities and Berry curvature values.

Given the pairing amplitude, the ground state is determined by  $V_m$  that reaches the maximum value. Plotting these  $V_m$  for different parameters  $k_F^2$  and  $b$  we observe a cascade of transitions between states with different  $m$  (see Fig.1). It turns out that the succession of different chiral phases is governed by the flux of pseudo-magnetic field through the Fermi surface

$$\Phi = \int_{FS} \mathbf{b} \frac{d^2k}{2\pi} = b \frac{k_F^2}{2}. \quad (23)$$

The boundaries between adjacent phases  $m$  and  $m+2$  are determined by the following equation

$$I_m\left(\frac{\Phi}{\sinh(ab)}\right) = I_{m+2}\left(\frac{\Phi}{\sinh(ab)}\right) e^{2ab} \quad (24)$$

Using the asymptotics of the Bessel functions one can show that for the local attraction ( $a \rightarrow \infty$ ) the boundaries are determined by the equation  $\Phi = m+1$ , while for the wide potential ( $a \rightarrow 0$ ) the boundaries are given by small- $a$  asymptotics  $\Phi = \sqrt{(m+1)(m+2)}$ . These properties explain the behavior of different phases in the phase diagram shown in Fig.1b at small and large  $ba$ .

We now consider the behavior near phase boundaries, the pairing interactions for the  $m$  and  $m+1$  orders are nearly equal, and they directly compete. On general symmetry grounds, at the phase boundaries these orders are expected to exhibit a type-I phase transition. In this situation, the phase diagram typically contains two distinct

superconducting phases, along with an intermediate region near the phase boundary where the two orders may coexist. Concretely, we focus on chiral superconducting pairing in the channels  $m$  and  $m+2$ , for which

$$\langle a_{\mathbf{k}} a_{-\mathbf{k}} \rangle \sim \Delta_1 e^{im\phi_{\mathbf{k}}} + \Delta_2 e^{i(m+2)\phi_{\mathbf{k}}}. \quad (25)$$

Within a mean-field framework, with an angle-dependent pairing interaction  $V_{\mathbf{k}\mathbf{k}'}$  that carries a geometric phase (as described above), this leads to the free energy

$$F(\Delta_1, \Delta_2) = -T \sum_{\mathbf{k}, i\omega_n} \text{Tr} \ln \begin{pmatrix} \epsilon_{\mathbf{k}} - i\omega_n & \Delta(\phi_{\mathbf{k}}) \\ \Delta^*(\phi_{\mathbf{k}}) & -\epsilon_{\mathbf{k}} - i\omega_n \end{pmatrix} + \frac{|\Delta_1|^2}{g_1} + \frac{|\Delta_2|^2}{g_2}, \quad g_1 = \nu V_m, \quad g_2 = \nu V_{m+2}, \quad (26)$$

where the gap function describes two competing pairing channels,  $\Delta(\phi_{\mathbf{k}}) = \Delta_1 e^{im\phi_{\mathbf{k}}} + \Delta_2 e^{i(m+2)\phi_{\mathbf{k}}}$ .

To obtain the dependence  $F(\Delta_1, \Delta_2)$ , we first carry out the (largely straightforward) summation over  $\omega_n$  and the radial integration over  $\mathbf{k}$  near the Fermi surface at fixed angle  $\phi_{\mathbf{k}}$ . Taking  $T = 0$  and, in the weak-coupling regime, assuming a small ratio  $\Delta/E_F \ll 1$ , this yields

$$F = \nu \oint \frac{d\phi_{\mathbf{k}}}{2\pi} |\Delta(\phi_{\mathbf{k}})|^2 \ln \frac{|\Delta(\phi_{\mathbf{k}})|^2}{E_F^2} + \frac{|\Delta_1|^2}{g_1} + \frac{|\Delta_2|^2}{g_2} \quad (27)$$

This free energy, which can be evaluated in a closed form [23], describes competition between the two chiral orders, predicting a first-order phase transition at each of the  $m-m+2$  phase boundaries.

A cascade of first-order transitions, which provides a clear experimental signature for this mechanism for chiral superconductivity, has several interesting implications:

One clear manifestation is oscillations of the critical temperature  $T_c$ , controlled by the Berry flux  $\Phi$  through the Fermi surface area and tunable via the carrier density. These oscillations are directly analogous to the seminal Little-Parks effect in conventional superconductors in a magnetic field, where the periodicity of  $T_c$  as a function of flux allows one to measure the superconducting flux

quantum  $hc/2e$ . In our case, the oscillations are governed by the commensurability of the Berry-curvature flux through the Fermi surface, realizing a quantum-geometry analog of the Little-Parks effect and providing a striking signature of chiral superconductivity.

Chiral superconducting phases with broken time-reversal symmetry are also expected to carry a finite magnetization. Estimating the orbital angular momentum per Cooper pair as  $\hbar m$ , one finds a corresponding magnetic-moment density of order  $\mu_B m |\Delta|^2$ . The dependence of the magnetization on  $m$  manifests itself in the way an external magnetic field  $H$  reshapes the phase diagram. Specifically, the energy of a phase with angular momentum  $m$  is lowered by  $\sim \mu_B m |\Delta|^2 H$ , favoring phases with larger  $m$  and suppressing those with smaller  $m$ . As a result, in the presence of a field  $H$ , each phase boundary in Fig. 1 is shifted inward (to smaller  $\Phi$ ) by an amount proportional to  $H$ .

Last but not least, in a spatially nonuniform system, first-order transitions between phases with different  $m$  will generate domains separated by boundaries that host chiral edge modes. The edge supercurrents carried by these modes can be directly probed by spatially resolved scanning magnetometry, while the chiral quasiparticles localized at the domain walls can be detected through signatures in chiral thermal transport.

In summary, this work demonstrates that Berry curvature in electronic bands qualitatively reshapes the superconducting pairing problem, giving rise to a cascade of chiral superconducting states characterized by quantized angular momentum  $m$ . Unlike conventional vortex physics driven by real-space magnetic fields, the Berry-curvature-induced pseudomagnetic field acts directly in momentum space, modifying the microscopic structure of Cooper pairs. As a result, superconducting order parameters acquire intrinsic phase winding on the Fermi surface, leading to a family of topologically distinct chiral states, manifested in a number of signatures readily detectable by state-of-the-art experimental techniques.

This work greatly benefited from discussions with Zhiyu Dong, Patrick Lee and Eli Zeldov.

- 
- [1] M. Tinkham, *Introduction to Superconductivity*, 2nd ed. (McGraw-Hill, New York, 1996).
- [2] E. H. Brandt, "The flux-line lattice in superconductors," *Rep. Prog. Phys.* **58**, 1465–1594 (1995).
- [3] G. Blatter, M. V. Feigel'man, V. B. Geshkenbein, A. I. Larkin, and V. M. Vinokur, "Vortices in high-temperature superconductors," *Rev. Mod. Phys.* **66**, 1125–1388 (1994).
- [4] G. W. Crabtree and D. R. Nelson, "Vortex physics in high-temperature superconductors," *Phys. Today* **50**(4), 38–45 (1997).
- [5] W.-K. Kwok, U. Welp, A. Glatz, A. E. Koshelev, K. J. Kihlstrom, and G. W. Crabtree, "Vortices in high-performance high-temperature superconductors," *Rep. Prog. Phys.* **79**, 116501 (2016).
- [6] G. Sundaram and Q. Niu, *Phys. Rev. B* **59**, 14915 (1999).
- [7] D. Xiao, M.-C. Chang, and Q. Niu, *Rev. Mod. Phys.* **82**, 1959 (2010).
- [8] G. Panati, H. Spohn, and S. Teufel, *Commun. Math. Phys.* **242**, 547 (2003).
- [9] S. Teufel, *Adiabatic Perturbation Theory in Quantum Dynamics* (Springer, 2003).
- [10] J. May-Mann, T. Helbig, and T. Devakul, "How pairing mechanism dictates topology in valley-polarized superconductors with Berry curvature," arXiv:2503.05697 (2025).
- [11] Z. Wang, L. Dong, C. Xiao, and Q. Niu, "Berry curvature effects on quasiparticle dynamics in superconduc-

- tors,” *Phys. Rev. Lett.* **126**, 187001 (2021).
- [12] O. Matsyshyn, G. Vignale, and J. C. W. Song, “Superconducting Berry curvature dipole,” arXiv:2410.21363 (2024).
- [13] M. Sato and Y. Ando, “Topological superconductors: a review,” *Rep. Prog. Phys.* **80**, 076501 (2017).
- [14] C. Kallin and J. Berlinsky, “Chiral superconductors,” *Rep. Prog. Phys.* **79**, 054502 (2016).
- [15] N. Read and D. Green, “Paired states of fermions in two dimensions with breaking of parity and time-reversal symmetries and the fractional quantum Hall effect,” *Phys. Rev. B* **61**, 10267–10297 (2000).
- [16] C. Nayak, S. H. Simon, A. Stern, M. Freedman, and S. Das Sarma, “Non-Abelian anyons and topological quantum computation,” *Rev. Mod. Phys.* **80**, 1083–1159 (2008).
- [17] T. Han *et al.*, “Signatures of chiral superconductivity in rhombohedral graphene,” *Nature* (2025), doi:10.1038/s41586-025-09169-7.
- [18] A. Ghazaryan, T. Holder, E. Berg, and M. Serbyn, “Multilayer graphenes as a platform for interaction-driven physics and topological superconductivity,” *Phys. Rev. B* **107**, 104502 (2023).
- [19] Y.-Z. Chou, J. Zhu, and S. Das Sarma, “Intravalley spin-polarized superconductivity in rhombohedral tetralayer graphene,” *Phys. Rev. B* **111**, 174523 (2025).
- [20] E. Viñas Boström, A. Fischer, J. B. Profe, J. Zhang, D. M. Kennes, and A. Rubio, “Phonon-mediated unconventional *s*- and *f*-wave pairing superconductivity in rhombohedral stacked multilayer graphene,” *npj Comput. Mater.* **10**, 163 (2024).
- [21] F. Gaggioli, D. Guerci, and L. Fu, “Spontaneous vortex-antivortex lattice and Majorana fermions in rhombohedral graphene,” *Phys. Rev. Lett.* **135**, 116001 (2025).
- [22] F. Paoletti, D. Guerci, G. Sangiovanni, U. F. P. Seifert, and E. J. König, “Topologically enabled superconductivity: possible implications for rhombohedral graphene,” arXiv:2504.13166 (2025).
- [23] Integration over the angle  $\phi_{\mathbf{k}}$  can be carried out using the identity

$$\int_0^{2\pi} |a + be^{i\phi}|^2 \ln(|a + be^{i\phi}|^2) \frac{d\phi}{2\pi} = (|a|^2 + |b|^2) (1 + \ln \max(|a|^2, |b|^2)) - ||a|^2 - |b|^2|. \quad (28)$$